JOURNAL OF MATERIALS SCIENCE 12 (1977) 884–892

The effects of flaws and voids on the shear properties of CFRP

N. L. HANCOX
Materials Development Division, AERE, Harwell, Oxon, UK

The shear properties of solid CFRP rods and tubes containing flaws and voids have been studied. The behaviour of tubes containing flaws parallel to the long axis can be described in terms of fracture mechanics, observed differences in critical flaw length between specimens being due to differing material properties. A qualitative theoretical explanation of the critical flaw length is given. The effect of flaws perpendicular to the long axis is dependent on the geometry of the specimen. Solids rods are not particularly sensitive to flaws. Voids reduce shear properties steadily until, at 5 vol % voids, values are only 30% of those for void-free CFRP. Previous theoretical treatments are not successful because the real void size and spatial distributions are unlike those assumed. It is suggested that fracture mechanics cannot be used to analyse the shear properties of materials containing voids.

1. Introduction

The shear properties of carbon fibre reinforced plastics (CFRP) are of considerable interest, since frequently they limit the application of the material. The present work is concerned with the influence of artificial flaws and voids arising from fabrication procedures on the shear behaviour of composites.

It is useful as a background to review previous work on the simple shear behaviour of CFRP. The longitudinal shear modulus G_c, shear strength τ_c, strain at failure, stress concentration β, in the matrix due to the presence of fibres, and torsional work of fracture, have been measured, see for instance [1–3]. Theoretical analysis [4, 5] has given the shear modulus and stress concentration factor as a function of fibre volume loading. Despite the differences between a real fibre composite structure and the models used, calculated and measured results are in good agreement. Attempts to calculate the shear strength, [6], have been much less successful.

Particularly puzzling has been the fact that for unidirectional HT–S fibre epoxy composites a shear strength greater than that of the matrix is obtained with 50 to 60 vol% of fibre. One contributing factor may be that the small quantities of resin around each fibre are in a quite different state, with different properties, from the bulk material. The structure in a small resin volume may be more ordered because the exotherm in the composite will be limited to the overall curing temperature by the presence of the good thermal conductivity fibres, the small distance, about 8 μm, between fibres may cause steric hinderance, and the accelerator may be preferentially absorbed on fibres. Another factor may be that the small spacing of fibres will tend to limit flaw growth in the matrix to one direction. The more ordered nature of the resin would be expected to lead to lower shear properties, but the constraint on flaw direction would oppose this tendency.

An alternative approach, based on energy considerations, has been provided by Reynolds and Hancox [2]. Assume that the actual maximum shear stress in the composite is $\beta\tau_{c,max}$. Then the shear strain energy/unit volume is given by

$$\frac{\alpha\beta^2(\tau_{c,max})^2}{G_c} \quad (1)$$

where α is a geometrical constant. For failure to occur this energy must be sufficient to initiate and propagate a crack. If the bond between the fibre

and matrix is sufficiently good that failure occurs in the resin rather than at the interface, then for failure,

$$\frac{\beta^2(\tau_{c,\max})^2}{G_c} = \frac{(\tau_r)^2}{G_r} \quad (2)$$

where r refers to the resin and $\beta = 1$ for the unreinforced resin. Equation 2 will be in error because the composite is assumed to be elastic to failure in shear, and as previously discussed it is not probable that the right-hand side will have the same value as it does for the bulk resin. Physically $\tau_{c,\max} > \tau_r$ because the good bonding between fibre and resin leads to a stiffer material, and until the requisite strain energy is stored in the composite failure cannot occur.

For other types of composite in which the bonding is less good and failure does not occur in the resin, Equation 2 applies but with another, unknown, quantity less than $(\tau_r)^2/G_r$ on the right-hand side. Since for these materials $\beta\tau_{c,\max}$ is reasonably constant and yet G_c increases with fibre content, the energy density to cause failure decreases with increasing fibre content, as would be expected if the area of weakness (i.e. fibre resin bond) is increased.

It is possible to express $\beta\tau_{c,\max}$ in terms of the fracture energy/unit area γ_c, and critical flaw length $2C$. Consider a flaw of length of $2C$ and depth t, existing between fibres in the surface region of a unindirectional composite. If the disturbance caused by this extends a distance C on either side of the flaw then following the procedure for deriving the Griffith's relation for tensile stressing, it is simple to show that for the crack to grow,

$$\beta\tau_{c,\max} = \sqrt{\left(\frac{2\gamma_c G_c}{C}\right)}. \quad (3)$$

This equation is approximate because of the non-elastic behaviour of real composites in torsion and the way the extent of the stress field has been approximated.

In this study the shear properties of pultruded and filament wound CFRP tubes and moulded solid rods containing artificial flaws were measured using a torsion rig and the results used to determine the critical flaw sizes for the various materials. If the flaw was parallel to the long axis of the tube the results could be analysed using a fracture mechanics approach. For flaws perpendicular to the long axis the tubular specimen should be regarded as a shell structure, and the geometry of the specimen has a greater influence than does the nature of the material.

To evaluate the influence of voids, unidirectional solid rod specimens prepared by various techniques that lead to differing volumes and distributions of voids, were tested in torsion and attempts made to account for the changes in strength and stiffness using theoretical models. It was found, as expected, that the void volume had a marked effect on shear behaviour but that it was not possible to account for this theoretically because the voids were irregular in shape and distribution.

2. Experimental work

Three types of nominally void-free specimens were produced from HT-S carbon fibre and a resin mix comprising 100 p.b.w. of liquid bisphenol A epoxy resin, 80 p.b.w. methyl nadic anhydride hardener and 2 p.b.w. benzyl dimethylamine accelerator, cured for 2 h at 120° C.

The pultruded tube with the fibres parallel to the long axis, contained 53 vol% fibre, had a mean diameter of 29 mm and a mean wall thickness of 1.5 mm. There was a tendency for delamination to occur when cutting the tube which was indicative of poor fibre wetting or incorrect curing in the pultrusion die, and this caused the material to have a relatively low shear strength.

The filament wound tube was reinforced in the hoop direction with 57.5 vol% fibre, had a mean diameter of 22 mm and a mean wall thickness of 1 mm. The outer surface was not machined in order to avoid fibre damage.

Solid specimens containing 60 vol% unindirectional fibre were moulded as square cross-section bars, cut into 180 mm lengths and the centre 150 mm turned to a diameter of 6.2 mm. For each of the above three types of specimen the void content was less than 1 vol%.

Flaws, about 0.2 mm to 0.3 mm deep, were cut in the solid rods, parallel to the long axis, using a specially supported scalpel. Cuts 0.5 mm wide, through the wall thickness, were made in the tubular specimens, parallel and perpendicular to the long axis.

Tubular specimens were cut into lengths between 65 mm and 95 mm and the 10 mm section at either end set into grooves, machined into paral-

TABLE I

Specimen type	Method of manufacture
V1	fibre soaked and degassed
V2	fibre soaked, not degassed
V3	fibre soaked in methyl ethyl ketone (MEK) and then heated for 10 mins. in resin and degassed
V4	as in V3 but no heating to remove MEK or final degassing

lel sided blocks of "Tufnol", with a filled, plasticised, epoxy resin. Solid rod specimens could be used without further preparation.

It was not considered practicable to produce a series of pultruded or wound tubes containing varying void volumes, and so four sets of 60 vol% HT-S carbon fibre solid rod specimens were wet moulded using the treatments listed in Table I, and subsequently machined to shape.

The torsional behaviour, to failure, of all specimens was measured as described in [1]. Modulus measurements on unflawed tubes were corrected for shear deflection in the end caps. The Nadai correction to the shear strength, required if the torque twist curve is non-linear, was only applied to solid specimens, since the departure from linearity in the case of most of the tubular ones was small.

The void contents of the solid bars were determined by measuring the ultrasonic velocity across the square ends of the specimens, at three locations, measurements being made in two orthogonal directions at each position. Apart from operational and calibration errors associated with a particular reading it is reasonable to expect the actual void content to vary from place to place in a specimen. The error bars shown in the figures reflect this. The mean void contents of large (1 g) sections of several bars were measured after testing by an acid digestion technique and found to agree within the error with the mean values determined ultrasonically.

Attempts were made to assess the void area in polished sections of specimen by scanning photographs of the section with a special microscope and photoelectric cell combination, but this was not found to be very successful because of the dispersed nature and small size of the voids and lack of contrast between voids and fibre.

3. Results and discussion

3.1. Flawed specimens

The shear modulus G_c and strength τ_c of unflawed solid rod and tubular specimens are listed in Table II. Four to six samples were used for most determinations. The low properties of the pultruded tube are noticeable and arise because the specimen was prone to delamination.

Fig. 1 shows that the shear strength of lengths of pultruded tube is substantially constant for gauge lengths between 23 mm and 75 mm.

The shear strength of flawed solid rods as a function of $C^{-1/2}$ where C is the half length of the flaw, parallel to the fibres in this material, is illustrated in Fig. 2. The errors have been calculated assuming a coefficient of variation of 7.9% [7]. The line is a least squares fit and indicates a critical flaw length of 2.0 mm, see Table II. However, in view of the scatter in the data, this is not particularly significant.

Figs. 3 and 4 show the shear strength of the pultruded and wound tubes as a function of $C^{-\frac{1}{2}}$. For the specimens in Fig. 3 the flaw is parallel to the long axis of the tube and, therefore, cuts a considerable number of fibres in the filament wound tube, but not in the pultruded one. In Fig.

TABLE II

Specimen	G (unflawed) GNm^{-2}	τ (unflawed) MNm^{-2}	Critical flaw length, 2C, mm. measured	
			Parallel to long axis	Perpendicular to long axis
Solid rod	5.26 ± 0.28	78 ± 5.1	2.0 ± 3.4	
			1.7	
Pultruded tube	2.9 ± 0.4	48	12.0 ± 2.6	5.0 ± 1.2
			4.0	0.8
Wound tube	4.1 ± 0.4	69 ± 4.2	0.9 ± 0.1	3.2 ± 0.4
			0.15	0.4
			2C, mm. calculated	
Solid rod			24.7	
Pultruded tube			35.8	
Wound tube				21.8

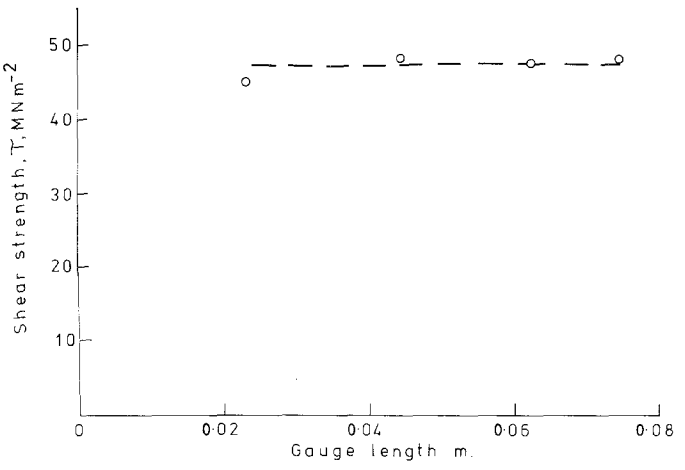

Figure 1 Shear strength versus length of unflawed pultruded tube.

4 the flaw is perpendicular to the long axis and so now cuts fibres in the pultruded but not in the wound tube. The points for zero shear strength in this figure correspond to flaw lengths equal to the circumferences of the tubes. Also included in Fig. 3 are the shear strengths of flawed solid rods. Each value has been multiplied by the ratio of the unflawed shear strength of the pultruded tube to that of the solid rod (48/78) to make the results comparable. The results for the solid rod and pultruded tube specimens in Fig. 3 fall into two regions, one where the strength falls rapidly with increasing flaw length, the other for smaller flaw sizes, where the strength is more or less constant.

For flaws parallel and perpendicular to the long axis critical lengths have been determined, allowing for the error expected in the unflawed shear strength, and are listed in Table II. The sizes are similar for the two materials when the flaw is perpendicular to the long axis, but very different when the flaw is parallel to the long axis. As in either case the flaws cut fibres in one type of specimen but not in the other, the behaviour when the flaw is perpendicular to the long axis is puzzling. Also included in Table II are the calculated values of the critical flaw size derived from Equation 3. A value for γ_c of about 16 kJ m^{-2}, for a unidirectional rod has been taken from [3], and it has

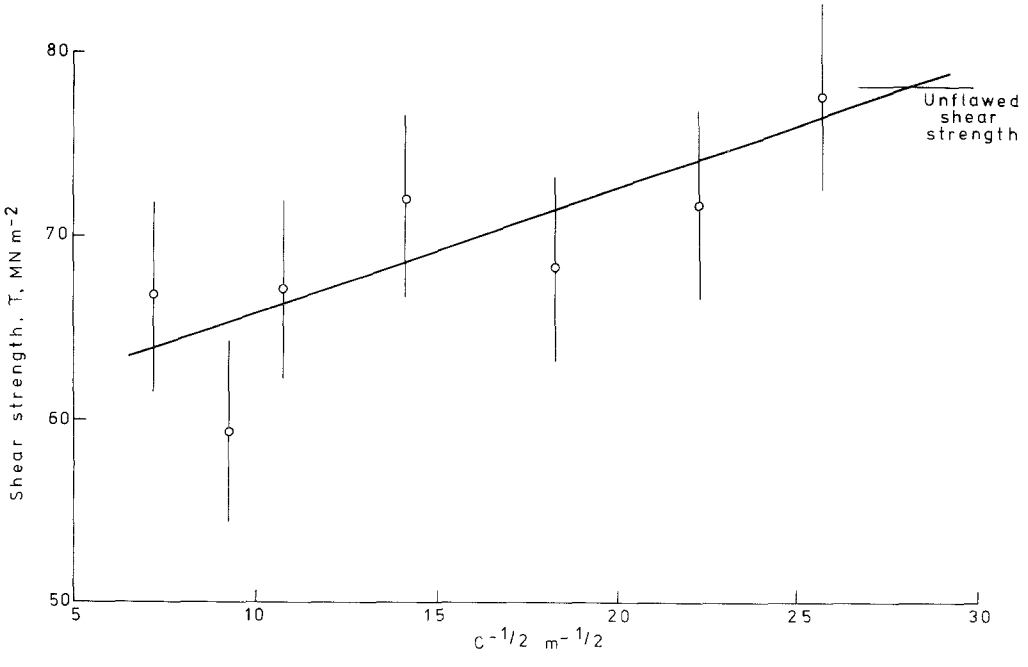

Figure 2 Shear strength of solid rods versus $C^{-\frac{1}{2}}$. 60 vol % HT-S fibre.

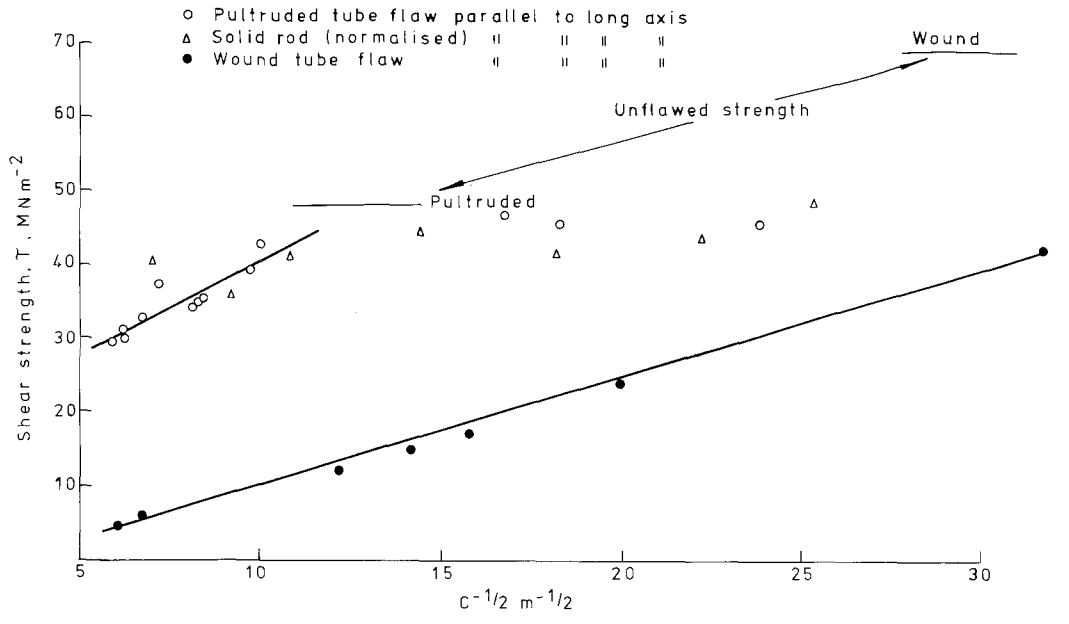

Figure 3 Shear strength versus $C^{-\frac{1}{2}}$.

been assumed that this value can be applied to all three materials. The discrepancies between measured and calculated values are large and probably due to the assumptions made in deriving Equation 3, and errors in determining γ_c, which because of the difficulty of finding the fracture surface area can be large.

The data are difficult to interpret because several effects are occurring. Firstly any tube with a cut or slit in it, particularly perpendicular to the long axis behaves as a shell and the ordinary torsion analysis cannot strictly be applied. It can be shown [8] that the maximum shear stress in an open channel section of constant thickness, such as an arc of a circle is given by

$$\tau_{max} = \frac{3T}{\phi^2 r^2 t} \quad (4)$$

where τ_{max} is the maximum shear stress at torque T, ϕ the angle subtended by the arc, r the mean

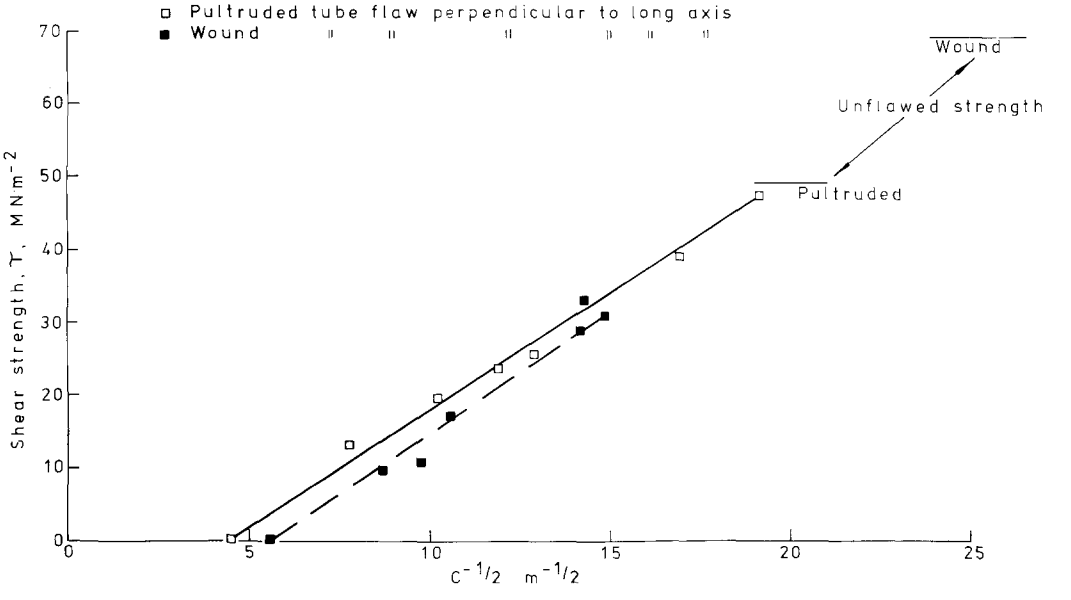

Figure 4 Shear strength versus $C^{-\frac{1}{2}}$.

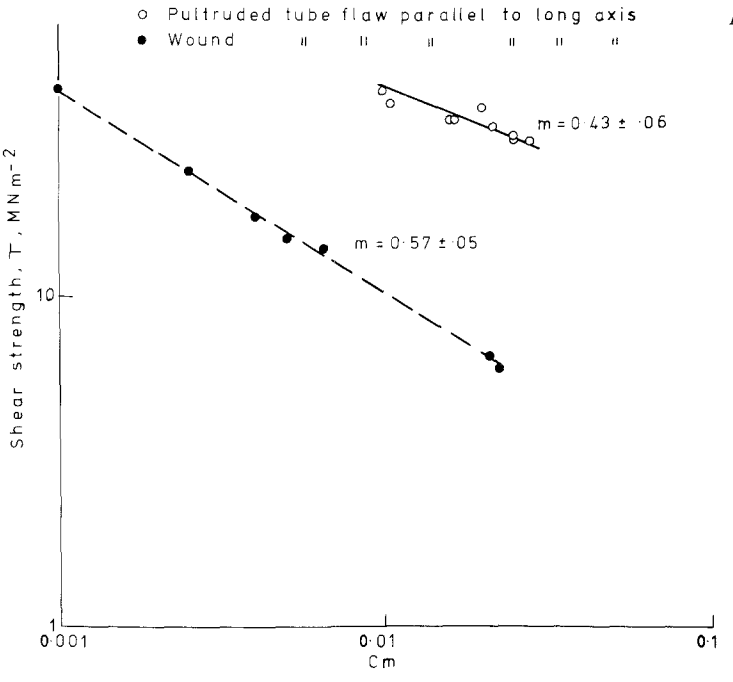

Figure 5 Shear strength versus *C*.

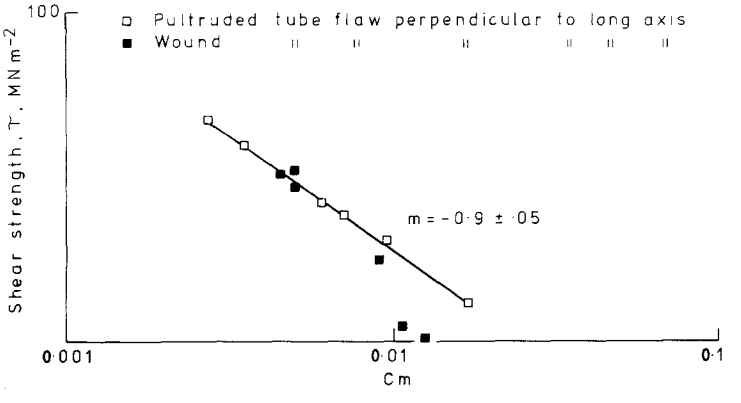

Figure 6 Shear strength versus *C*.

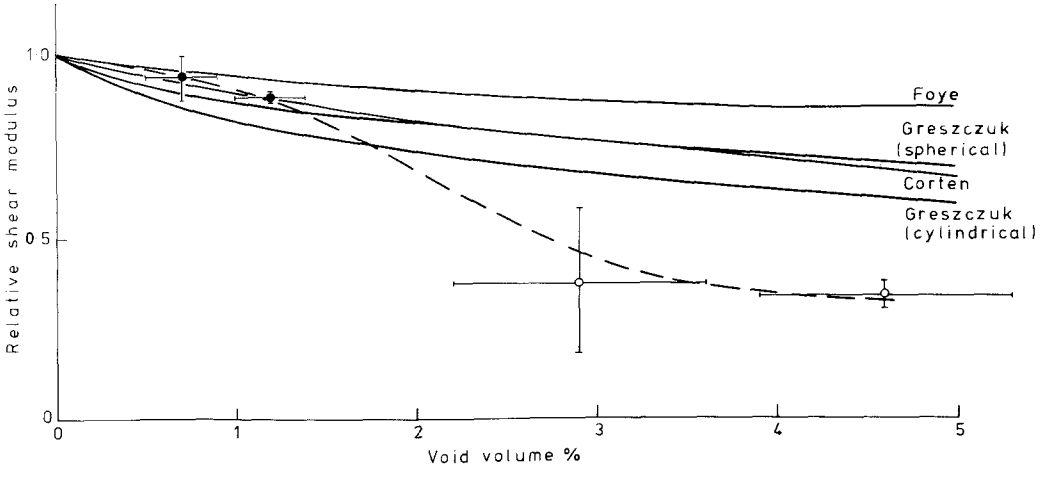

Figure 7 Relative shear modulus versus void volume.

radius of the arc and t the thickness. Use of Equation 4 with measured values of T for failure of tubes with parallel or perpendicular flaws yielded values of τ_{max} well in excess, by up to 100%, of the unflawed strength. It was concluded that this approach failed because of the stiffening action of the material on either side of the flaw, and that simple torsion theory, though not accurate especially for tubes containing perpendicular flaws, was the best approximation available.

Secondly the materials in the pultruded and wound tubes are different in that the fibre resin bond in the latter is much better than in the former. This will effect their response to flaws and stress concentration.

It is suggested that when the flaw is perpendicular to the long axis of the tube, geometrical effects (departure from simple torsion theory) override those of stress concentration at the flaw tip irrespective of material properties, and the critical flaw length is a function of geometry rather than the material. With the flaw parallel to the long axis of the tube, departures from simple theory are presumed to be less, and over a range of flaw lengths, constant. Now the differences in critical sizes and behaviour must be accounted for in terms of differing material properties. The wound tube behaves in a brittle manner, while for the pultruded tube stress concentration can be relieved at the flaw tip because of poor bonding until the flaw is 10 mm or more in length. The solid rod would have been expected to behave like the wound tube as it had a good shear modulus and strength. The difference may be due to some effect of the material in the core modifying crack propagation or because of the way in which flaws were produced.

The stress intensity factor, K_{II}, for mode II deformation such as occurs here can be written as

$$K_{II} = \tau(\pi C)^{1/2} \quad (5)$$

where τ is the shear stress at infinity.

Wu [9] has analysed experiments on the fracture of glass fibre laminates by taking logarithms of both sides of Equation 5 and plotting $\log \tau$ versus $\log C$. If the slope is, within the error, -0.5 he concluded that fracture mechanics methods were applicable.

Accordingly the data for tubes with flaws parallel to the long axis were replotted in Fig. 5 and with the flaws perpendicular to the long axis in Fig. 6. In the former case the slopes are -0.57 ± 0.05 and -0.43 ± 0.06 for wound and pultruded tubes respectively. It is believed that these are sufficiently close to -0.5 to be able to conclude that the behaviour is governed by fracture mechanics. In Fig. 6 only one line with a slope of -0.9 ± 0.05 has been drawn for two sets of data, and it is concluded that in this case behaviour is governed by the geometry of this specimen.

3.2. Specimens containing voids

The shear properties of solid unidirectional rods containing up to 5 vol% voids were measured by twisting the rods to failure, in the manner already described. Relative (with respect to the initial zero void value) shear moduli and strengths are shown as a function of void content in Figs. 7 and 8. Modulus and strength values in shear for the void free material were taken as 5.4 GN m^{-2} and 50 MN m^{-2}, respectively. The horizontal bars represent the standard error of the mean void content, and

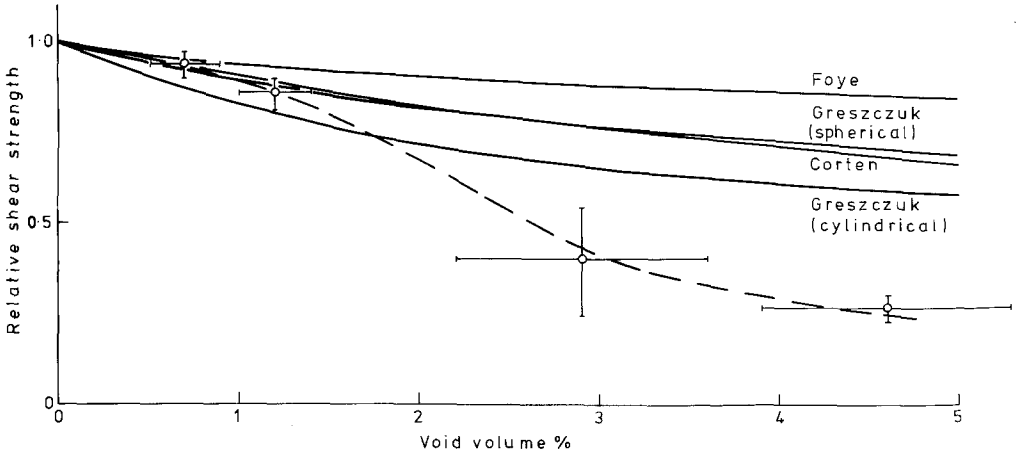

Figure 8 Relative shear strength versus void volume.

the vertical ones the range of a modulus or strength measurement. The angular displacement at failure was approximately constant at 18°.

The mechanical properties show little spread with the exception of those for specimens with a void content at 2.9 vol %. It should be remembered that the range of void contents studied here (0 to 5 vol %) is less than has been the case in previous work and hence the error in void content may be more noticeable.

Various theoretical predictions of the effects of voids on shear modulus and strength are included in Figs. 7 and 8. Foye [10] considered cylindrical voids parallel to the fibres in the composite and equated strain energy in this material to that in a long hollow cylinder of void free material whose outer surface displacements correspond to those of a uniform shear strain while the inner surface is stress free. He thus obtained G_v, the shear modulus of the voidy material, in terms of G and the void content. The shear strength variation on this model can only be calculated approximately since although the angular deflection at failure is known, the torque twist curve is not linear to failure.

Greszczuk [11] considered a cubic array of spherical voids and a rectangular array of cylindrical ones. He used a strength of materials approach, neglecting stress concentration, and assumed that the maximum shear stress occurred at a section where the peripheries of the adjacent voids are closest. The variation of shear modulus with void content was calculated from the strength results in a manner analagous to that in which strength was calculated from modulus by Foye [10].

Corten [12] assumed that fracture mechanics could be applied to a composite material and that the effective crack length was proportional to the cube root of the void volume fraction V. Using Equation 5 and assuming that the critical stress intensity factor is constant gives

$$\tau = C V^{-1/6}. \quad (6)$$

The constant C, was chosen to give a fit to the first data point. Modulus results were determined in the same way as strengths were determined using the results of Foye [10]. It is interesting to note the similarity between the result of Corten [12] and those of Greszczuk [11] for spherical voids.

It can be seen in Figs. 7 and 8 that up to a void volume of about 1.4 vol % either of the models of Greszczuk [11] or Corten [12] predict behaviour

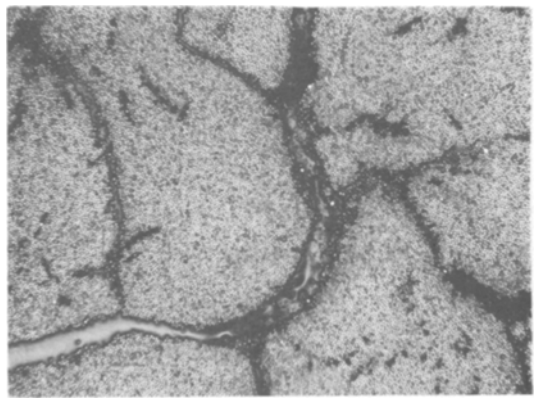

Figure 9 Section of failed 2.9% voids specimen, × 160.

quite well. Above this void content measured properties fall off much more rapidly than any of the theories indicate, and by 5 vol % voids both strength and modulus have been reduced to about 30% of the void-free values. The analysis of Greszczuk [11] could be modified to allow for stress concentration effects but it is likely that in practice these would be relieved because of poor bonding in the vicinity of voids.

A more likely explanation for the fall off in properties concerns the types of voids and their distribution. The general pattern of voids can best be seen by viewing polished sections of surface at an angle of 45° with the unaided eye. The lowest void content specimens had a core of fine voids with a few towards the edge, while in the 1.1 vol % void specimens, voids were still small, often regions of 50 μm in dimension, but now extending more uniformly across the surface. With the third type of specimen, voids 2.9 vol %, voids were more heavily concentrated at tow boundaries throughout the specimen. This is illustrated in Fig. 9; the clear feature in the left-hand lower corner is a crack, starting at the surface. The highest void content specimen showed many well dispersed void areas, 50 to 100 μm in dimension, and often aligned. A careful examination indicated that shear cracks originating at the surface frequently travelled through areas of high void concentration; see Fig. 9, and Fig. 10 which is of a 1.1 vol % void content specimen.

Polished longitudinal sections of composite showed that in all cases, but particularly for the 2.9 vol % specimens, voids tended to be line defects sometimes several millimetres in length.

In view of these observations it is hardly surprising that theories based on regular arrays of spheri-

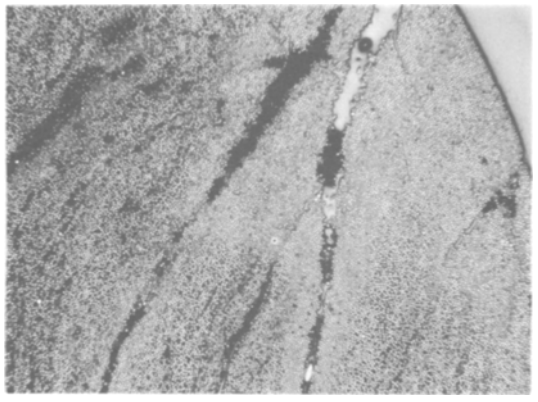

Figure 10 Section of failed 1.1% voids specimen, × 160.

cal or cylindrical voids or dispersions of the former fail to account for the experimental results. Voids concentrated in tow boundaries and meeting the surface would be particularly damaging as one or more of these lines would provide an ideal plane of weakness for longitudinal shear failure. Presumably the extra voids in the 4.6 vol% specimen more than compensate for the fact that concentration at tow boundaries is less than with 2.9 vol% void content samples.

The failure of the theory based on fracture mechanics [12] to predict accurately above about 1.4 vol% voids indicates that, while it may be possible to analyse the effects of artifical flaws such as cuts in a tube by fracture mechanics, this may not be so for microvoids introduced during manufacture. This might be because even in a system with good overall bonding, voids, unlike cuts, introduce local regions of poor bonding which allow stress relief to occur before cracking.

4. Conclusion

Aspects of the behaviour under torsion of flawed rods and tubes and material containing voids have been examined. Strength measurements on tubes containing cuts are difficult to analyse because of the interaction of material and geometrical properties, but it is concluded that fracture mechanics can almost certainly be applied if the flaw is parallel to the long axis of the tube. Critical flaw lengths were approximately 1 mm and 12 mm for wound and pultruded tubes respectively the difference being due to differing fibre resin bond strengths in the two materials. Solid rods were not very sensitive to surface flaws. The theoretical treatment developed accounts qualitatively for the results. The effect of flaws perpendicular to the long axis was similar for either material and due to geometrical properties rather than material considerations.

Voids have a serious degrading effect on shear modulus and strength, reducing properties to 30% of their void free value at 5 vol% voids. Theoretical treatments fail to predict the extent of the decrease as the actual and assumed sizes and distributions of voids are very different. There is some evidence that, unlike the case for flaws, the effect of voids cannot be analysed by the use of fracture mechanics, probably because voids involve areas of bad fibre resin bonding at which delamination can occur.

Acknowledgement

This work was carried out with the support of the Procurement Executive, Ministry of Defence.

References

1. N. L. HANCOX, *J. Mater. Sci.* 7 (1972) 1030.
2. W. N. REYNOLDS and N. L. HANCOX, *J. Phys. D.* **4** (1971) 1747.
3. N. L. HANCOX, AERE-R (1975).
4. D. F. ADAMS and D. R. DONER, *J. Comp. Mater* **1** (1967) 4.
5. M. D. HEATON, *J. Phys. D.* **2** (1968) 1039.
6. B. W. ROSEN and N. F. DOW, "Fracture", Vol. 7, edited by H. Liebowitz (Academic Press, New York, 1972) pp. 612–672.
7. N. L. HANCOX, AERE-R 7763 (1974); *J. Mater. Sci.* **11** (1975) 560.
8. S. P. TIMOSHENKO and D. H. YOUNG, "Strength of Materials", 3rd Edn. (Van Nostrand, Princetown, 1962).
9. E. M. WU, "Composite Materials Workshop", I, edited by S. W. Tsai, J. C. Halpin and N. J. Pagano, (Technomic, Stamford, 1968) pp. 20–43.
10. R. L. FOYE, A.I.A.A., 3rd Aerospace Science Meeting, New York, paper 66–143 (1966).
11. L. B. GRESZCZUK, 22nd S.P.I. Conference Washington, USA, 20A–1–10, (1967).
12. H. T. CORTEN, "Fundamental Aspects of Fibre Reinforced Plastic Composites", R. T. and H. S Schwartz, (Interscience, New York, 1968) pp. 89–107.

Received 9 September and accepted 4 October 1976.